Radboud Repository

Radboud University Nijmegen

PDF hosted at the Radboud Repository of the Radboud University Nijmegen

The following full text is a publisher's version.

For additional information about this publication click this link.
http://hdl.handle.net/2066/92071

Please be advised that this information was generated on 2017-12-06 and may be subject to change.

Soft Matter

PAPER

Microfluidic production of monodisperse functional o/w droplets and study of their reversible pH dependent aggregation behavior†

Wolfgang-Andreas C. Bauer,[a] Jurij Kotar,[b] Pietro Cicuta,[b] Robert T. Woodward,[c] Jonathan V. M. Weaver[d] and Wilhelm T. S. Huck*[ae]

We report the use of microfluidics for the production of monodisperse oil-in-water droplets functionalized by a pH responsive branched co-polymer surfactant. The droplet functionality facilitates the reversible aggregation of the micron-sized droplets into macroscopic engineered emulsions in response to solution pH changes. Co-injection of dye-loaded and non-dyed droplets into acidic water yields bi-colored dumbbell-shaped aggregates that disassemble into their constituent droplet building blocks upon an increase in pH. Optical tweezers are used to study and quantify the pH dependent interactions of individual droplets.

Introduction

Microdroplets in microfluidics have attracted enormous attention in chemical and biological sciences in recent years.[1] One key advantage of the microfluidic approach compared to conventional bulk emulsification techniques is the high level of control that is achievable over droplet monodispersity. Flow-focussing devices[2] can routinely generate water-in-oil (w/o) or oil-in-water (o/w) droplets with volumes in the fL to nL range at frequencies of several kHz, making the method a powerful platform for combinatorial assays and high-throughput screening. Furthermore, droplets can be precisely manipulated on-chip with robust methods in place for droplet fusing,[3] splitting,[4] sorting[5] and storing,[6] and their contents can be mixed,[7] extracted and analyzed.[8] By integrating multiple functional modules, lab-on-a-chip devices capable of performing numerous tasks can be produced.[9] Although this is a relatively young field of scientific research microdroplets in microfluidics exhibit widespread applications in various areas, including chemical synthesis,[10] particle production[11] and cell-based assays.[12]

In order to generate stable emulsion droplets, whether in microfluidic devices or in bulk, the liquid–liquid interface usually requires stabilization by surfactants. Among the plethora of emulsifiers that can be found in literature a recent development is the introduction of stimuli responsive properties within the surfactant.[13] These 'smart' surfactants typically facilitate switching between a stabilizing and a non-stabilizing state. Hence, their application is limited to stabilization and controlled demulsification, thus triggering the release of the internal droplet phase. Very recently the concept of 'emulsion engineering' was reported.[14,15] This approach uses a new type of responsive branched co-polymer surfactant based on methacrylic acid (MAA) and poly(ethylene glycol) methacrylate (PEGMA). The surfactant efficiently stabilizes polydisperse o/w droplets prepared using standard bulk homogenization techniques at basic pH. Under these conditions the droplets exist as conventional free-flowing emulsion dispersions. In contrast, under acidic conditions, aggregation of emulsion droplets into macroscopic engineered emulsion structures is triggered. This assembly process is reversible and the droplets retain their structural integrity during the assembly/disassembly process.

However, using conventional bulk emulsification methods it is not possible to control the fabric of aggregates due to inherent droplet polydispersity. In this paper we employ state-of-the-art microfluidic techniques to produce microdroplets with polydispersities in the range of only 1.5% (standard deviation of diameter divided by mean diameter). Due to their particularly narrow size distribution they can be considered monodisperse. We use these droplets as uniform building blocks for the formation of assembled soft materials with defined microstructure and study quantitatively pH dependent droplet–droplet interactions *via* optical tweezers.

Results and discussion

In Fig. 1 the schematics of our approach, combining microfluidic droplet production with emulsion engineering, are given.

[a]University of Cambridge, Department of Chemistry, Melville Laboratory for Polymer Synthesis, Lensfield Road, Cambridge, CB2 1EW, UK. E-mail: w.huck@science.ru.nl
[b]University of Cambridge, Cavendish Laboratory and Nanoscience Center, JJ Thomson Avenue, Cambridge, CB3 0HE, UK
[c]University of Liverpool, Department of Chemistry, Donnan Laboratories, Crown Street, Liverpool, L69 7ZD, UK
[d]Imperial College London, Departments of Materials and Bioengineering, Exhibition Road, London, SW7 2AZ, UK
[e]Radboud University Nijmegen, Institute for Molecules and Materials, Heyendaalseweg 135, Nijmegen, 6525 AJ, The Netherlands
† Electronic supplementary information (ESI) available: Details of device design, videos of Fig. 2 and 4. See DOI: 10.1039/c1sm05087g
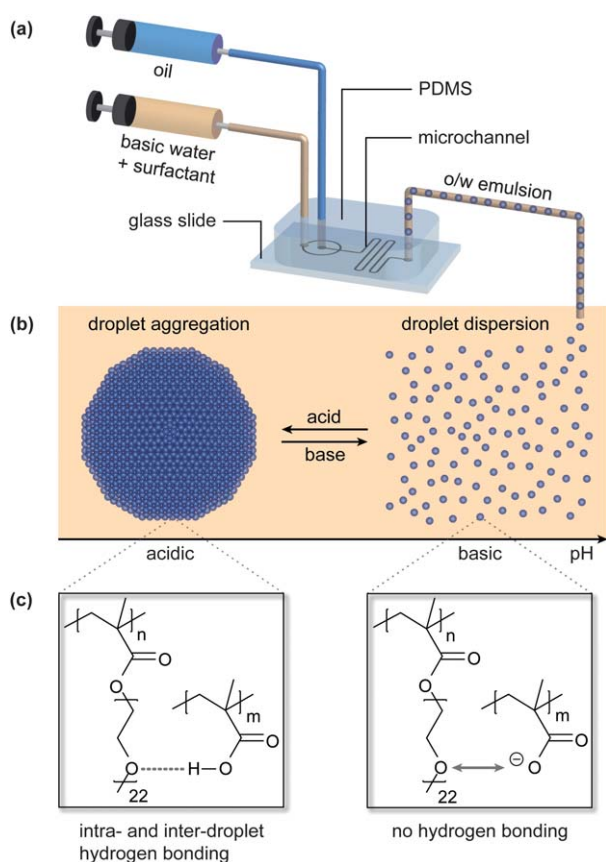
Fig. 1 Schematics of a microfluidic approach to smart droplets. (a) By injecting oil and basic water containing a pH responsive surfactant into a microfluidic device monodisperse o/w droplets with predefined surface functionality are produced on-chip. (b) Under basic conditions those droplets form a dispersion, but the addition of acid triggers a reversible aggregation. (c) The pH dependent droplet behavior is governed by switchable interactions between MAA and PEG moieties of the emulsifier. At basic pH values the deprotonation of MAA groups prevents hydrogen bonding and aggregation, whereas under acidic conditions hydrogen bonds between PEG and protonated MAA residues are formed. Inter-droplet hydrogen bonding causes a reversible droplet self-assembly.

Fig. 1(a) illustrates the formation of o/w droplets by the injection of oil and basic water containing the pH responsive MAA/PEGMA surfactant (MAA/ethylene glycol (EG) 1 : 1) into a microfluidic device. The controlled nature of the process allows for the production of monodisperse droplets whose surface functionality is predefined by the smart emulsifier. In Fig. 1(b) a schematic representation of the pH dependent behavior of the o/w droplets is shown. Under basic conditions a dispersion of non-interacting droplets is formed due to the simultaneous electrostatic and steric stabilization afforded by the PEGMA and MAA residues, respectively. Upon addition of acid the droplets self-assemble into higher-order engineered emulsion structures due to inter-droplet hydrogen bonding between MAA and EG residues. These assembled structures exist only under acidic conditions, because they disassemble back into dispersion when base is added to the system. Fig. 1(c) shows the structural formulas of the PEGMA and MAA residues, which are responsible for the pH responsive droplet behavior, under basic

and acidic conditions. At basic pH values the MAA groups are deprotonated and cannot form hydrogen bonds with poly(ethylene glycol) (PEG) moieties. In contrast, under acidic conditions the MAA units are protonated and hydrogen bonding with PEG residues takes place. These interactions are not restricted to groups at the surface of the same droplet (intra-droplet hydrogen bonding) but can also occur between MAA and PEG moieties of adjacent droplets (inter-droplet hydrogen bonding) leading to droplet assembly. Since the building blocks are held together only by transient secondary interactions the resultant aggregates are dynamic by nature and the assembly process is completely reversible.[14,15]

Microfluidic production of monodisperse functional droplets

In a first step, we produced pH responsive droplets using microfluidic techniques (Fig. 2). We manufactured a hybrid device comprising a poly(dimethylsiloxane) (PDMS) top part and a glass bottom plate by standard soft lithographic methods.[16] In order to overcome the inherent hydrophobicity of PDMS and assure an effective wetting of the microchannel walls with the continuous aqueous phase we applied a hydrophilic coating prior to droplet generation. In this context, we built up a polyelectrolyte multilayer (PEM) onto the channel wall using an automated layer-by-layer (LbL) surface modification technique which is described in detail elsewhere.[17] This procedure involves the alternate flushing of the microchannel with poly(allylamine hydrochloride) (PAH) and poly(sodium 4-styrenesulfonate) (PSS) solutions and creates hydrophilic surfaces that are stable over months. After device modification we injected n-dodecane as dispersed phase and basic water (pH 10) containing 2.0% w/v of the stimuli responsive MAA/PEGMA surfactant (MAA/EG 1 : 1).[14]

In Fig. 2(a) the stable formation of uniform o/w droplets at a frequency of 3.2 kHz at the flow-focusing region is shown. Constant flow rates of 100 μl h⁻¹ and 300 μl h⁻¹ were applied for dodecane and water, respectively. Under these conditions the droplets passed smoothly through the microchannel (Fig. 2(b)). After collecting the resultant emulsion for 2 hours a sample volume of ca. 5 μl was transferred into a storage device. The micrograph in Fig. 2(c) reveals a hexagonal close-packed monolayer of droplets formed inside the reservoir. The monodispersity of the droplets was quantified by determining the diameter distribution of 1101 droplets, as shown in Fig. 2(d). Distortions of the measurement due to compression and deformation of the droplets could be excluded as the reservoir height of ca. 150 μm exceeded the droplet diameter by far. Droplet size analysis yielded a narrow diameter distribution with a mean value of 26.6 μm. The standard deviation of 0.4 μm is only about 1.5% of the average value, indicating a high level of droplet monodispersity.

In order to test droplet functionality we performed proof-of-principle aggregation studies. For this purpose we loaded the generated o/w emulsion into a piece of polyethylene (PE) tubing and injected it afterwards at a constant flow rate of 70 μl h⁻¹ into open reservoirs which contained water at different pH values. When the sample is streamed into basic water at a pH value of 10 a dispersion of individual droplets was found (Fig. 2(e)). In contrast, the micrograph in Fig. 2(f) depicts the creation of
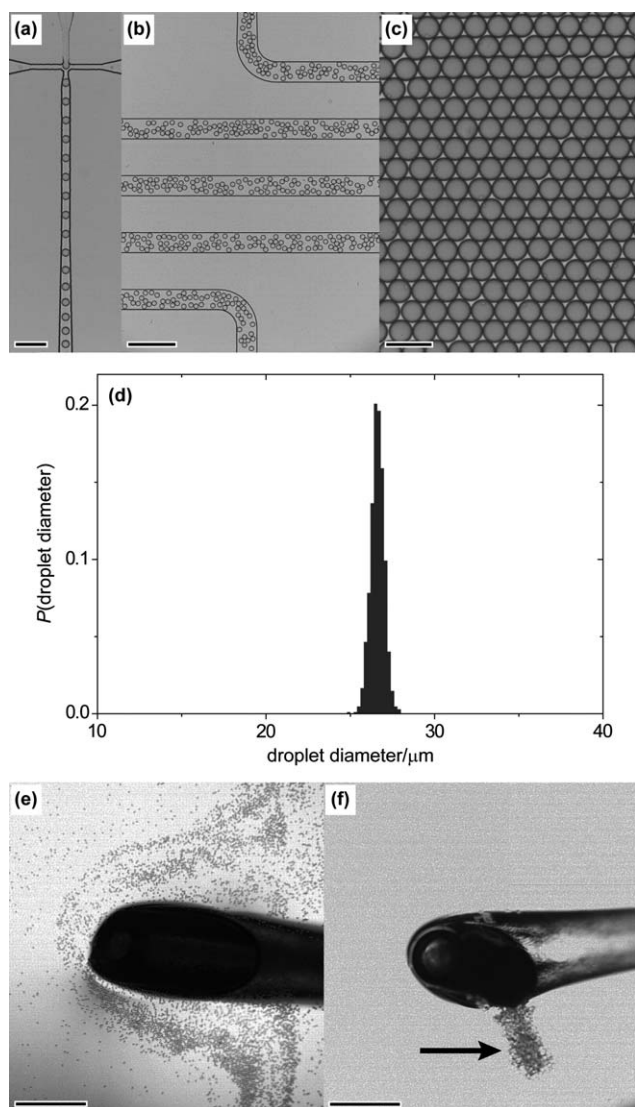
Fig. 2 Microfluidic production of monodisperse dodecane-in-water droplets and proof-of-principle aggregation test. The micrographs (a) and (b) depict the formation of o/w droplets stabilized by a pH responsive surfactant at the flow-focusing region and their passage through the microfluidic device, respectively. (c) This micrograph shows the hexagonal close-packed monolayer formed by the produced droplets in a storage device. (d) Diameter distribution reveals a high level of droplet monodispersity. Micrographs of the injection of the emulsion sample into (e) water at pH 10 and (f) water at pH 2 prove that droplets build up aggregates (see arrow) only under acidic conditions. Scale bars denote (a) 100 μm, (b) 250 μm, (c) 50 μm, (e), (f) 1 mm.

a droplet aggregate (see arrow) in acidic water at pH 2. These results prove that we are able to generate monodisperse droplets capable of forming either dispersions or assembled structures depending on the pH value of the continuous phase.

Reversible formation of bi-colored dumbbell-shaped droplet aggregates

In another bulk experiment we produced bi-colored dumbbell-shaped droplet aggregates and induced their disassembly

afterwards (Fig. 3). For this we used the aforementioned 26.6 μm dodecane-in-water emulsion droplets and freshly prepared colored o/w droplets formed on-chip from dodecane containing 0.5% w/v of the dye 1,4-bis(butylamino) anthraquinone (Solvent Blue 35) and the basic surfactant solution described above at a flow rate ratio of 100 μl h^{-1}–300 μl h^{-1}. The resultant blue droplets were monodisperse and exhibited a mean diameter of 28.1 ± 0.4 μm. The photograph in Fig. 3(a) shows the stained (right) and the unstained emulsion stored in glass vials.

We drew both samples into syringes which we brought into an upright position. As dodecane droplets have a lower density than the aqueous solution they were enriched at the top and could be extruded together with only a minimum amount of the continuous phase through PE tubing. Stained and unstained droplets were simultaneously co-injected next to each other into acidic water (pH 2), both at a flow rate of 500 μl h^{-1}. Spherical aggregates formed instantaneously and fused to each other yielding bi-colored dumbbells with a dark (dye-loaded) and a bright (non-dyed) half (Fig. 3(b)). The micrograph in Fig. 3(c) reveals that
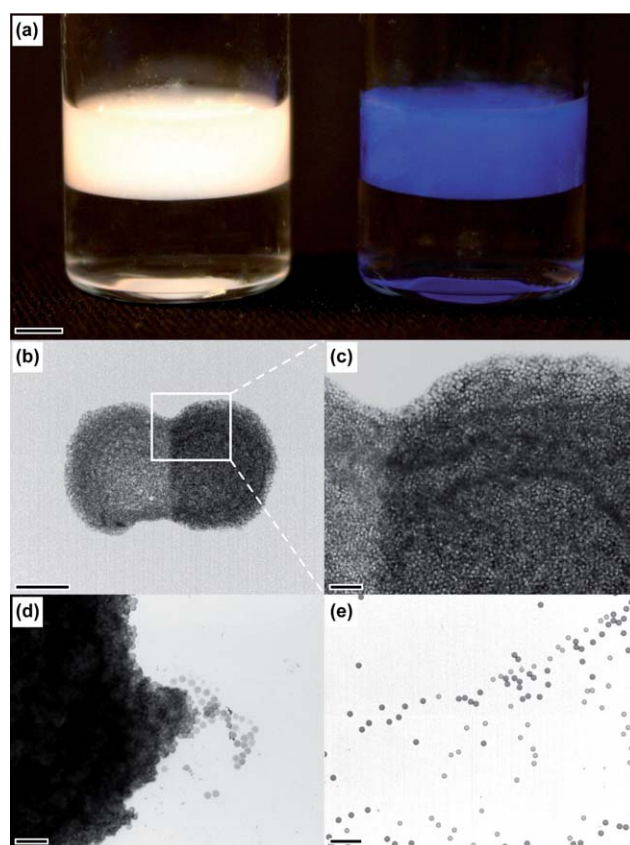

Fig. 3 Reversible formation of a bi-colored droplet aggregate. (a) This photograph shows samples of a dye-loaded (right) and a non-dyed dodecane-in-water emulsion stored in glass vials. The micrographs (b) and (c) depict a dumbbell-shaped aggregate formed under acidic conditions. It exhibits a dark and a bright half composed of close-packed dodecane droplets that are dyed or unstained, respectively. (d) In this micrograph the beginning disassembly of the aggregate upon the successive addition of basic water is shown. (e) After complete disaggregation a dispersion of non-interacting, dyed and non-dyed droplets can be found, as depicted in this micrograph. Scale bars denote (a) 2.5 mm; (b) 1 mm; (c)–(e) 100 μm.

these aggregates consist of close-packed emulsion droplets. However, due to the rapidity of the aggregation process the droplets did not have time to arrange into an ordered crystalline-like pattern but were kinetically trapped. Again, these assemblies were stable under acidic conditions but disassembled into their constituent droplet building blocks upon the addition of basic water (pH 12). As shown in Fig. 3(d) the disassembly process started off at the periphery of the engineered emulsion structure with the release of individual droplets and small droplet clusters. After several minutes the aggregates were completely disassembled and a dispersion of non-interacting stained and unstained droplets was observed (Fig. 3(e)). In this study we demonstrate that we are able to produce aggregates composed of uniform droplets, join them together forming macroscopic objects with a defined overall morphology and control their disassembly into distinct monodisperse droplets.

Optical tweezers analysis of pH dependent droplet interaction

Having studied engineered emulsions in bulk experiments we addressed pH dependent inter-droplet aggregation behavior on a single droplet level using optical tweezers.[18] Optical tweezers are most commonly used to manipulate colloidal particles, but it has been shown that they are valuable tools for noninvasive, contactless manipulation of many other micron-sized objects, such as bacteria[19] and red blood cells.[20] Concerning emulsion systems optical tweezers have been used to deform[21] and transport droplets[22] as well as to induce droplet fusion.[23]

In this series of experiments we used an optical tweezers setup consisting of a laser focused through a water immersion objective, which allows for trapping of objects in a reservoir from below. In order to explore exclusively inter-droplet adhesion we aimed for three-dimensional (3D) trapping in the reservoir lumen avoiding interferences with water-reservoir interfaces. However, due to the repulsive upward photon pressure force it is not possible with our setup to trap droplets with a lower density than the continuous phase in 3D. Hence, instead of generating pure dodecane-in-water

droplets we used a 1 : 2 (v/v) mixture of dodecane and 1-bromo-pentane as the dispersed phase. These droplets have a slightly higher density than water so that the photon pressure can be balanced allowing 3D droplet trapping. A microfluidic device coated with a PEM[17] was used and flow rates of 75 μl h^{-1} for the oil mixture and 250 μl h^{-1} for water (pH 10) containing 2.0% w/v of the MAA/PEGMA surfactant (MAA/EG 1 : 1) were applied. We produced o/w droplets at a frequency of 2.6 kHz. Subsequent droplet size analysis revealed a mean diameter of 21.0 ± 0.3 μm and a high level of monodispersity. We studied the effect of the pH value of the continuous phase on droplet interaction by analyzing basic and acidic droplet samples via optical tweezers. The basic sample was prepared by adding 2 μl of the droplet phase to 1 mL of water (pH 12) and transferring 16 μl of the resultant emulsion into a reservoir with a height of 120 μm. The same procedure was followed for the acidic sample but instead of basic water we used a freshly prepared 1.0 wt% solution of glucono-δ-lactone (GδL) in water (pH 12). GδL is a sugar compound well-known to hydrolyze in water yielding gluconic acid which gradually lowers the pH value of the solution over time.[15,24] The in situ pH reduction using GδL delayed droplet aggregation and gave us enough time to transfer the sample to the reservoir and to elevate the droplets before droplet adhesion to the bottom of the reservoir could occur.

The quantitative analysis of pH dependent droplet interaction via optical tweezers is illustrated in Fig. 4. In each sample we used two optical traps to capture a pair of droplets and to lift them with the laser beam to the middle of the reservoir lumen. The optical trap enforces a rotationally symmetric harmonic potential in the plane of focus, and a free droplet rapidly moves so that its center is at the trap position. While the left trap remained stationary the movement of the right one was precisely controlled by a computer program. In Fig. 4(a) the distance between the optical traps is plotted against time. Inserted micrographs illustrate the positions of the trapped o/w droplets; red dots indicate trap positions. Via correlation filtering and sub-pixel interpolation, the center of the droplets is established with a precision of about 1 nm on each frame. At first, a trap distance of 20 μm was set pushing droplets tightly together and
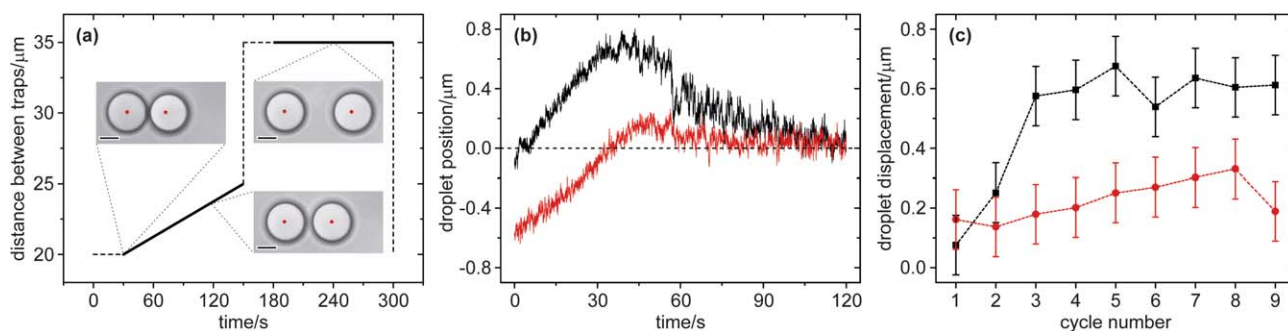

Fig. 4 Quantitative analysis of pH dependent droplet interactions via optical tweezers. (a) Distance between optical traps and positions of trapped droplets in the course of an approach/retract cycle. The left trap is kept stationary while the right one is moved back and forth; red dots in inserted micrographs indicate trap positions. Droplets are brought into tight contact before they are steadily separated. The position of the quasi-stationary left droplet is recorded (bold line) during retract and in state of separation for displacement measurement and trap calibration, respectively. Scale bars in micrographs denote 10 μm. (b) Position of the left droplet during retract under acidic (black curve) and basic conditions (red curve). The left droplet moves linearly alongside the right droplet to its rest position (dashed line). Due to droplet adhesion the left droplet exceeds this position before it looses contact and relaxes back to its rest position. The distance between maximum displacement of the left droplet and its rest position, and hence inter-droplet adhesion, is considerably higher under acidic than under basic conditions. (c) Evolution of displacement values of the left droplet over time for the acidic (black curve) and the basic (red curve) sample. Droplet displacement remains constant within the error under basic conditions. In the acidic sample droplet displacement rises with decreasing pH value within the first three cycles and stays at an elevated plateau afterwards.

displacing the quasi-stationary left droplet slightly out of its rest position. After an equilibration time of 30 s the trap distance was steadily increased to 25 μm over a period of 120 s while the position of the left droplet along the movement axis was recorded. Subsequently, the distance between the traps was abruptly increased to 35 μm. After another 30 s of equilibration the position of the left droplet was recorded for 120 s in order to calibrate the trap. This approach/retract cycle was run nine times for both samples. The computer-controlled manipulation of droplets *via* optical tweezers was facilitated by the high level of monodispersity in our droplet sample produced by microfluidic techniques, which ensured that droplet–droplet contact areas and forces acting on the droplets were consistent and comparable for different droplet pairs.

Fig. 4(b) exhibits representative graphs for the position of the left droplet during the retract of the right droplet for a droplet pair under acidic (black curve) and basic conditions (red curve). Both graphs show three distinct sections: (i) linear change of position with time when the left droplet follows the right one to its rest position (dashed line), (ii) transgression of the rest position due to droplet–droplet interactions and (iii) relaxation to the rest position. Comparison between both curves reveals that droplet displacement and thus adhesive interactions between droplets are significantly higher under acidic conditions than in the basic sample. Differences in droplet positions at the starting point are the result of slightly unequal droplet diameters in the range of 0.5 μm. In Fig. 4(c) the maximum displacement of the left droplet in each retract cycle is plotted for the acidic (black curve) and the basic sample (red curve). Within the error the displacement remains constant over time under basic conditions with an average value of 0.225 ± 0.067 μm. In contrast, for the acidic sample the displacement values increase strongly for the first three cycles before reaching a plateau value with a mean displacement of 0.605 ± 0.043 μm approximately 14.5 min after adding GδL to the continuous phase. This hydrolysis time corresponds to a pH value of 4.3 ± 0.1, well below the pK_a value of PMAA (5.6),[25] indicating that a fairly high degree of protonation of the MAA moieties of the surfactant chains is needed in order to attain maximum inter-droplet attraction.

Based on these average displacement values we calculated droplet adhesion forces. In our optical tweezers experiments the trapping potential can be locally described by a harmonic potential. We calibrated the corresponding trap stiffness by recording the thermal fluctuations of the left o/w droplet for 2 min at a constant trap distance of 35 μm in each approach/retract cycle (Fig. 4(a)). Details of trap calibration are described elsewhere.[26] Trap stiffness was consistent and independent of pH with an average value of 1.77 ± 0.56 pN μm^{-1}. Multiplication of this number with the average displacement of the left droplet during retraction of the right one yields a maximum adhesion force of 0.40 ± 0.25 pN under basic and 1.07 ± 0.42 pN under acidic conditions. The ranges of error were calculated by adding the relative errors of trap stiffness and droplet displacements.

Experimental

Materials

Unless stated otherwise, all chemicals were obtained from Sigma-Aldrich and used as received without further purification. Milli-Q water (Millipore) was used throughout all of the experiments.

Microfluidic device fabrication

Microfluidic devices were fabricated by conventional soft lithographic techniques.[16] Microchannel architectures were designed with AutoCAD (AutoDesk) and transferred to high resolution photomasks fabricated on transparencies (Circuit Graphics). The negative photoresist SU-8 2025 (MicroChem) was spin-coated onto 3 inch silicon wafers (Compart Technology) and patterned using a MJB4 mask aligner (Süss MicroTec). Development was accomplished by immersion into 1-methoxy-2-propyl acetate.

A commercially available Sylgard 184 PDMS kit (Dow Corning), containing the pre-polymer and a cross-linker, was used in the recommended ratio of 10 : 1 (w/w). The mixture was poured on top of the patterned silicon wafers and degassed. After curing at 80 °C for 10 h the PDMS cast was cut and peeled off the wafers. Inlets and outlets were stamped out using a biopsy punch (Kai Industries) with an outer diameter of 1 mm. The microfluidic devices were assembled by joining the PDMS cast and a microscope glass slide. Bonding strength was provided by pre-treating both contact surfaces with oxygen plasma for 8 s in a Femto plasma cleaner (Diener electronic).

Storage devices were fabricated following the same process. Instead of patterned wafers, microscope cover slips glued onto glass slides were used as casting molds.

Hydrophilic surface modification of microchannels

Directly after device assembly a PAH-PSS-PAH-PSS PEM was deposited onto the microchannel walls by an automated LbL method as described elsewhere.[17] Solutions of NaCl (AnalaR) in water (0.1 M) as well as of PAH ($M_w \approx 56\,000$) and PSS ($M_w \approx 70\,000$), both 0.1% w/v in 0.5 M aqueous NaCl solution, were prepared. Segments of these solutions, separated by air plugs, were loaded into a piece of PE tubing (Becton Dickinson). Using a PHD 2000 syringe pump (Harvard Apparatus) they were sequentially flushed through the microchannel at a constant flow rate of 50 μl h^{-1}.

Microfluidic experiments

The synthesis of the pH responsive branched co-polymer surfactant is described in detail elsewhere.[14] Water at a pH value of 10 containing 2.0% w/v of the MAA/PEGMA surfactant (MAA/EG 1 : 1) was used as continuous phase. The basic pH value of this solution was adjusted by the addition of 1.0 M sodium hydroxide solution and monitored with a SevenEasy pH meter (Mettler Toledo). Three oil phases were applied to form o/w droplets: (i) pure dodecane, (ii) dodecane stained with 0.5% w/v of the dye Solvent Blue 35 and (iii) a dodecane/1-bromopentane 1 : 2 (v/v) mixture.

Water and oil phases were injected into microfluidic devices *via* PE tubes (Becton Dickinson). In all microfluidic experiments PHD 2000 syringe pumps (Harvard Apparatus) were used to inject liquids at constant flow rates between 75 μl h^{-1} and 300 μl h^{-1}.

Droplet formation on-chip as well as emulsion samples inside storage devices were imaged using a monochrome Phantom v7.2 camera (Vision Research) attached to an IX71 inverted microscope (Olympus). The frequency of droplet formation and the

droplet diameter distribution were calculated using LabVIEW 8.2 (National Instruments).

Droplet aggregation experiments in bulk

Emulsion droplets were injected through PE tubes (Becton Dickinson) into open reservoirs containing water at acidic or basic pH, adjusted by the addition of 1.0 M hydrochloric acid and 1.0 M sodium hydroxide solution, respectively. A SevenEasy pH meter (Mettler Toledo) was used to measure the pH values of the aqueous solutions. The flow rates of droplet streams were kept constant at either 70 μl h^{-1} or 500 μl h^{-1} by PHD 2000 syringe pumps (Harvard Apparatus). Micrographs were obtained using a Phantom v7.2 camera (Vision Research) attached to an IX71 inverted microscope (Olympus).

Optical tweezers analysis

The optical tweezers setup consists of a PYL-1-1064-LP laser (IPG Photonics, $\lambda = 1064$ nm, $P_{max} = 1.1$ W) focused through an Achroplan IR 63x/0.90 W water immersion objective (Zeiss), trapping from below. The laser beam was steered *via* a pair of AA.DTS.XY-250@1064 nm acousto-optic deflectors (AA Opto-Electronic) controlled by custom-built electronics, allowing (by time sharing) multiple trap generation with sub-nanometre position resolution. Instrument control and data acquisition were performed by custom software. Calibration of trap stiffness was carried out by measuring the thermal displacements of the trapped droplets.[26] Reservoirs were built by placing a Secure-Seal imaging spacer (Sigma-Aldrich) with a diameter of 13 mm and a height of 120 μm between a glass slide and a microscope cover slip.

Conclusions

In summary, we successfully combined the concepts of engineered emulsions with the benefits of the microfluidic approach. In microfluidic devices we produced monodisperse, functional o/w droplets stabilized by a pH responsive co-polymer surfactant. Aggregation driven by inter-droplet hydrogen bonding into macroscopic structures and disaggregation back into dispersion were controlled using a simple pH trigger. We quantitatively analyzed pH dependent interactions between individual droplets using optical tweezers. In well-defined approach/retract cycles we brought droplets into close contact and separated them again. Based on the measurement of droplet displacements we demonstrated that droplet–droplet adhesion is significantly higher under acidic than under basic conditions and exhibits a time evolution when the pH value of the continuous phase is continuously lowered *in situ* over time. The results presented here provide valuable new insight into pH dependent inter-droplet interactions and open the way for new experiments in emulsion engineering, where droplets of different sizes and composition can be combined on-chip and allowed to assemble into reversible superstructures.

Acknowledgements

References

1 G. M. Whitesides, *Nature*, 2006, **442**, 368–373; S.-Y. Teh, R. Lin, L.-H. Hung and A. P. Lee, *Lab Chip*, 2008, **8**, 198–220; A. B. Theberge, F. Courtois, Y. Schaerli, M. Fischlechner, C. Abell, F. Hollfelder and W. T. S. Huck, *Angew. Chem., Int. Ed.*, 2010, **49**, 5846–5868.
2 S. L. Anna, N. Bontoux and H. A. Stone, *Appl. Phys. Lett.*, 2003, **82**, 364–366; S. L. Anna and H. C. Mayer, *Phys. Fluids*, 2006, **18**, 121512.
3 D. R. Link, E. Grasland-Mongrain, A. Duri, F. Sarrazin, Z. Cheng, G. Cristobal, M. Marquez and D. A. Weitz, *Angew. Chem., Int. Ed.*, 2006, **45**, 2556–2560; L. M. Fidalgo, C. Abell and W. T. S. Huck, *Lab Chip*, 2007, **7**, 984–986; N. Bremond, A. R. Thiam and J. Bibette, *Phys. Rev. Lett.*, 2008, **100**, 024501.
4 D. R. Link, S. L. Anna, D. A. Weitz and H. A. Stone, *Phys. Rev. Lett.*, 2004, **92**, 054503; L. Menetrier-Deremble and P. Tabeling, *Phys. Rev. E: Stat., Nonlinear, Soft Matter Phys.*, 2006, **74**, 035303.
5 Y.-C. Tan, J. S. Fisher, A. I. Lee, V. Cristini and A. P. Lee, *Lab Chip*, 2004, **4**, 292–298; K. Ahn, J. Agresti, H. Chong, M. Marquez and D. A. Weitz, *Appl. Phys. Lett.*, 2006, **88**, 264105; Y.-C. Tan, Y. L. Ho and A. P. Lee, *Microfluid. Nanofluid.*, 2008, **4**, 343–348.
6 F. Courtois, L. F. Olguin, G. Whyte, D. Bratton, W. T. S. Huck, C. Abell and F. Hollfelder, *ChemBioChem*, 2008, **9**, 439–446; F. Courtois, L. F. Olguin, G. Whyte, A. B. Theberge, W. T. S. Huck, F. Hollfelder and C. Abell, *Anal. Chem.*, 2009, **81**, 3008–3016.
7 H. Song, M. R. Bringer, J. D. Tice, C. J. Gerdts and R. F. Ismagilov, *Appl. Phys. Lett.*, 2003, **83**, 4664–4666; H. Song, J. D. Tice and R. F. Ismagilov, *Angew. Chem., Int. Ed.*, 2003, **42**, 767–772; H. Song and R. F. Ismagilov, *J. Am. Chem. Soc.*, 2003, **125**, 14613–14619.
8 L. M. Fidalgo, G. Whyte, D. Bratton, C. F. Kaminski, C. Abell and W. T. S. Huck, *Angew. Chem., Int. Ed.*, 2008, **47**, 2042–2045; L. M. Fidalgo, G. Whyte, B. T. Ruotolo, J. L. P. Benesch, F. Stengel, C. Abell, C. V. Robinson and W. T. S. Huck, *Angew. Chem., Int. Ed.*, 2009, **48**, 3665–3668.
9 T. Thorsen, S. J. Maerkl and S. R. Quake, *Science*, 2002, **298**, 580–584; S. Haeberle and R. Zengerle, *Lab Chip*, 2007, **7**, 1094–1110.
10 Z. T. Cygan, J. T. Cabral, K. L. Beers and E. J. Amis, *Langmuir*, 2005, **21**, 3629–3634; T. Hatakeyama, D. L. Chen and R. F. Ismagilov, *J. Am. Chem. Soc.*, 2006, **128**, 2518–2519; H. Song, D. L. Chen and R. F. Ismagilov, *Angew. Chem., Int. Ed.*, 2006, **45**, 7336–7356.
11 Z. Nie, S. Xu, M. Seo, P. C. Lewis and E. Kumacheva, *J. Am. Chem. Soc.*, 2005, **127**, 8058–8063; S. Xu, Z. Nie, M. Seo, P. Lewis, E. Kumacheva, H. A. Stone, P. Garstecki, D. B. Weibel, I. Gitlin and G. M. Whitesides, *Angew. Chem., Int. Ed.*, 2005, **44**, 724–728; T. Nisisako and T. Torii, *Adv. Mater.*, 2007, **19**, 1489–1493; W. Li, H. H. Pham, Z. Nie, B. MacDonald, A. Guenther and E. Kumacheva, *J. Am. Chem. Soc.*, 2008, **130**, 9935–9941; S. Dubinsky, H. Zhang, Z. Nie, I. Gourevich, D. Voicu, M. Deetz and E. Kumacheva, *Macromolecules*, 2008, **41**, 3555–3561; Q. Xu, M. Hashimoto, T. T. Dang, T. Hoare, D. S. Kohane, G. M. Whitesides, R. Langer and D. G. Anderson, *Small*, 2009, **5**, 1575–1581.
12 A. Huebner, M. Srisa-Art, D. Holt, C. Abell, F. Hollfelder, A. J. de Mello and J. B. Edel, *Chem. Commun.*, 2007, 1218–1220; A. Huebner, L. F. Olguin, D. Bratton, G. Whyte, W. T. S. Huck, A. J. de Mello, J. B. Edel, C. Abell and F. Hollfelder, *Anal. Chem.*, 2008, **80**, 3890–3896; Q. Boedicker, L. Li, T. R. Kline and R. F. Ismagilov, *Lab Chip*, 2008, **8**, 1265–1272; J. Clausell-Tormos, D. Lieber, J.-C. Baret, A. El-Harrak, O. J. Miller, L. Frenz, J. Blouwolff, K. J. Humphry, S. Köster, H. Duan, C. Holtze, D. A. Weitz, A. D. Griffiths and C. A. Merten, *Chem. Biol.*, 2008, **15**, 427–437; E. Brouzes, M. Medkova, N. Savenelli, D. Marran, M. Twardowski, J. B. Hutchison, J. M. Rothberg, D. R. Link, N. Perrimon and M. L. Samuels, *Proc. Natl. Acad. Sci. U. S. A.*, 2009, **106**, 14195–14200.
13 A. M. Mathur, B. Drescher, A. B. Scranton and J. Klier, *Nature*, 1998, **392**, 367–370; S. Fujii, E. S. Read, B. P. Binks and S. P. Armes, *Adv. Mater.*, 2005, **17**, 1014–1018; S. Fujii, Y. Cai, J. V. M. Weaver and S. P. Armes, *J. Am. Chem. Soc.*, 2005, **127**, 7304–7305; Y. Liu, P. G. Jessop, M. Cunningham, C. A. Eckert and C. L. Liotta, *Science*, 2006, **313**, 958–960; R. T. Woodward, R. A. Slater, S. P. Rannard, A. I. Cooper, B. J. L. Royles, P. H. Findlay and J. V. M. Weaver, *Chem. Commun.*, 2009, 3554–3556.

14 J. V. M. Weaver, R. T. Williams, B. J. L. Royles, P. H. Findlay, A. I. Cooper and S. P. Rannard, *Soft Matter*, 2008, **4**, 985–992; J. V. M. Weaver, S. P. Rannard and A. I. Cooper, *Angew. Chem., Int. Ed.*, 2009, **48**, 2131–2134; R. T. Woodward and J. V. M. Weaver, *Polym. Chem.*, 2011, **2**, 403–410.

15 R. T. Woodward, L. Chen, D. J. Adams and J. V. M. Weaver, *J. Mater. Chem.*, 2010, **20**, 5228–5234.

16 D. Qin, Y. Xia and G. M. Whitesides, *Adv. Mater.*, 1996, **8**, 917–919; D. C. Duffy, J. C. McDonald, O. J. A. Schueller and G. M. Whitesides, *Anal. Chem.*, 1998, **70**, 4974–4984.

17 W.-A. C. Bauer, M. Fischlechner, C. Abell and W. T. S. Huck, *Lab Chip*, 2010, **10**, 1814–1819.

18 S. M. Block, *Nature*, 1992, **360**, 493–495; A. Ashkin, *Proc. Natl. Acad. Sci. U. S. A.*, 1997, **94**, 4853–4860.

19 S. M. Block, D. F. Blair and H. C. Berg, *Nature*, 1989, **338**, 514–518; R. Dasgupta, S. K. Mohanty and P. K. Gupta, *Biotechnol. Lett.*, 2003, **25**, 1625–1628.

20 Y.-Z. Yoon, J. Kotar, G. Yoon and P. Cicuta, *Phys. Biol.*, 2008, **5**, 036007; Y.-Z. Yoon, J. Kotar, A. T. Brown and P. Cicuta, *Soft Matter*, 2011, **7**, 2042–2051.

21 A. D. Ward, M. G. Berry, C. D. Mellor and C. D. Bain, *Chem. Commun.*, 2006, 4515–4517.

22 R. M. Lorenz, J. S. Edgar, G. D. M. Jeffries and D. T. Chiu, *Anal. Chem.*, 2006, **78**, 6433–6439.

23 M. Hase, A. Yamada, T. Hamada, D. Baigl and K. Yoshikawa, *Langmuir*, 2007, **23**, 348–352; J. Tang, A. M. Jofre, R. B. Kishore, J. E. Reiner, M. E. Greene, G. M. Lowman, J. S. Denker, C. C. C. Willis, K. Helmerson and L. S. Goldner, *Anal. Chem.*, 2009, **81**, 8041–8047.

24 Y. Pocker and E. Green, *J. Am. Chem. Soc.*, 1973, **95**, 113–119.

25 S. Fisher and R. Kunin, *J. Phys. Chem.*, 1956, **60**, 1030–1032.

26 M. Leoni, J. Kotar, B. Bassetti, P. Cicuta and M. C. Lagomarsino, *Soft Matter*, 2009, **5**, 472–476.